ASEAN Journal of Chemical Engineering 2024, Vol. 24, No. 2, 210 – 228

Exploring Microwave-Assisted Pyrolysis of *Sargassum* sp. for Optimal Process Parameters and Product Insights

Teta Fathya Widawati [1]
Muhammad Fuad Refki [1]
Rochmadi [1,3]
Arief Budiman [*,1,2]
[1] *Center for Energy Studies, Universitas Gadjah Mada, Sekip K1A, Yogyakarta 55281, Indonesia*
[2] *Department of Chemical Engineering, Universitas Gadjah Mada, Jl. Grafika No. 2, Kampus UGM, Yogyakarta, 55281, Indonesia*
[3] *Carbon Research Group, Universitas Gadjah Mada, Jl. Grafika No. 2, Kampus UGM, Yogyakarta, 55281, Indonesia*[*]
*e-mail: abudiman@ugm.ac.id

Submitted 13 April 2024 *Revised* 19 July 2024 *Accepted* 28 July 2024

Abstract. Microwave-assisted pyrolysis (MAP) offers a promising alternative to fast pyrolysis for scaling up biomass conversion processes, facilitating accelerated reactions without significant temperature elevation. This study investigated the optimum process parameters for MAP of *Sargassum* sp., the predominant macroalgae in Indonesia. Parameters explored included *Sargassum* sp. particle sizes (10-40, 40-70, 70-100, >100 mesh), final temperatures (300, 350, 400, 450 °C), and coconut activated carbon (CAC)-to-feedstock ratios (1:2, 1:1, 3:2), with CAC acted as a microwave absorber. Experimental results indicated that the highest volatile yield (57.64%) occurred at a 40-70 mesh particle size and a final temperature of 450 °C, yielding bio-oil and gas at 24.88% and 32.76%, respectively. Increasing CAC loading enhanced bio-oil and char yields while reduced gas production, with a 1:1 ratio, yielded an optimal calorific value. Bio-oil density ranged from 0.9557 to 0.9968 g/mL. Gas chromatography-mass spectrometry (GC-MS) analysis revealed significant sterol derivatives and butanoic acid in the bio-oil, with lower concentrations of N-aromatic compounds. Fourier-transform infrared spectroscopy (FTIR) identified key peaks characteristic of aromatic (1400 and 1500 cm^{-1}), carbonyl (1700 cm^{-1}), C-N bonds (2100-2200 cm^{-1}), amide and amine (3300-3400 cm^{-1}), and hydroxyl and carboxylic acid (3450 cm^{-1}). These findings underscored the efficacy of MAP in achieving high volatile yields at relatively moderate temperatures compared to conventional methods. Moreover, butanoic acid's presence in the bio-oil highlighted its potential as a valuable resource for safe food preservation and chemical synthesis. However, detecting sterol derivatives and complex N-aromatic compounds suggested incomplete decomposition at 350 °C.

Keywords: Bio-oil, Macroalgae, Microwave absorber, Parameters, Volatiles

INTRODUCTION

Pyrolysis is one of the thermochemical processes employed to convert biomass into energy products and value-added chemicals (Wibowo *et al.*, 2023; Wang *et al.*., 2018). The pyrolysis process, also known as thermal cracking, involves the decomposition of

DOI: 10.22146/ajche.12871

feedstock at high temperatures (>400 °C) in the absence of oxygen (O_2) (Ali-Ahmad *et al.*., 2020). Pyrolysis can be categorized into slow pyrolysis, fast pyrolysis, flash pyrolysis, and microwave-assisted pyrolysis (MAP) (Gupta and Mondal, 2022; Yang *et al.*, 2019; Jesus *et al.*, 2019; Ethaib *et al.*, 2020).

Microwave-assisted pyrolysis (MAP) is a promising option for mass scaling up alongside fast pyrolysis. With the assistance of microwaves, pyrolysis reactions can be accelerated without drastically increasing the operating temperature. Microwaves have wavelengths in the infrared (IR) and radio range, from 1 mm to 1 m, with a frequency range of 300 MHz to 30 GHz (Ethaib *et al.*, 2020). Microwave radiation causes the disintegration of molecules in biomass, which can accelerate the breakdown of biomass cell walls.

The products of MAP, including bio-oil, char, and gas, have various applications. For instance, bio-oil contains aliphatic, phenols, aromatics, and polyaromatic hydrocarbons, which can be utilized as biofuel (Jamilatun *et al.*, 2019). Bio-oil can be upgraded to gasoline or biodiesel through hydrotreating processes (Pradana *et al.*, 2017; Wang *et al.*, 2021). Furthermore, value-added chemicals such as phenols, acids, carbonyls, and formaldehyde augment their applicability in various industries, including flavor enhancement, dye production, antibacterial agents, and texture modification (Jamilatun *et al.*, 2019). Pyrolysis gas contains H_2, hydrocarbons (C_1-C_4), CO, and CO_2, which can be purified and upgraded into fuels and reactants for other chemical processes (Zhang *et al.*, 2023). With its porous structure and high carbon content, char is suitable as a soil conditioner to improve soil quality (Yadav *et al.*, 2016).

Given their prevalence in various shallow coastal waters in Indonesia, macroalgae is a potentially abundant raw material for MAP products. The high diversity of macroalgae, including species found on the Southern coast of Gunungkidul, Yogyakarta, makes it a suitable candidate for raw material for pyrolysis. *Sargassum* is the most dominant genus found in the southern coast of Gunungkidul and other seawaters in Indonesia (Sodiq and Arisandi, 2020).

Sargassum is a brown alga (Phaeophycae) with a high carbohydrate content, ranging from 46.59% to 50.98% (Salosso, 2019). To date, it has been used mainly as supplementary food, feed, and biofertilizer. Unlike Ulva lactuca, *Sargassum* sp. is not utilized as a functional food material, which lowers its economic value. For these reasons, *Sargassum* is a suitable candidate for a pyrolysis raw material to produce pyrolysis products, especially bio-oil.

MAP efficiency is influenced by several factors, such as feedstock characteristics, operating temperature, and microwave absorber (Ethaib *et al.*, 2020). Temperature significantly affects the yield of pyrolysis products, with higher pyrolysis temperatures resulting in increased yields of bio-oil and gas (Amrullah *et al.*, 2024). Additionally, temperature influences the distribution of compounds within the bio-oil. Particle size is directly related to the surface area of biomass; smaller particle sizes result in larger surface areas. A larger surface area enhances heat transfer rate through convection and conduction, theoretically leading to higher heating rates.

Essentially, the MAP process, with the assistance of microwave waves (frequency of 2.45 GHz or 0.0016 eV), cannot break the chemical bonds (C-C, C-O, C-H, O-H) in the cell walls of biomass feedstock. Therefore, MAP requires a microwave absorber with high dielectric constant and dielectric loss

tangent to convert microwaves into heat energy, such as coconut activated carbon (CAC) (Ethaib *et al.*, 2020; Mushtaq *et al.*, 2014).

A proper absorber has high dielectric constant and dielectric loss tangent. The dielectric constant, or relative permittivity, describes the ability of an absorber to resist the flow of microwave waves and store them. The dielectric constant describes the polarity of a compound, with higher values indicating higher polarity. The dielectric constant consists of real (ε′) and imaginary (ε″) components. Dielectric loss tangent (tanδ) is the ratio of the imaginary permittivity (ε″) to the real permittivity (ε′). The dielectric loss tangent represents the amount of energy dissipated as heat.

Materials with a high tanδ value can dissipate microwave waves into heat (Chuayjumnong *et al.*, 2020). CAC has a higher tanδ value, specifically 1.65 (Omar *et al.*, 2011). This value is higher compared to coal (0.02–0.08), carbon black (0.35–0.83), carbon nanotube (0.25–1.14), SiC nanotube (0.58–1.00), oil palm fiber (0.08), oil palm shell activated carbon (0.4), aspen bark (0.22), and pine bark (0.18) (Torgovnikov, 1993; Marland *et al.*, 2001; Atwater and Wheeler, 2004; Lin *et al.*, 2008; Yao *et al.*, 2008; Omar *et al.*, 2011).

For an absorbent to be an effective microwave absorber, it must have characteristics such as non-reactivity, a large surface area, porosity, and high pore volume (Widawati *et al.*, 2024). For low-frequency microwaves, it is better to use a mesoporous absorber. CAC meets these criteria due to its inherent non-reactivity and low cost.

Enhanced absorption is influenced by the impedance matching between the microwave absorber (Z_{in}) and air (Z_0), high microwave attenuation, and low minimum reflection loss (RL) (Cheng *et al.*, 2020; Chitaningrum *et al.*, 2022). The large pore volume of CAC lowers its effective permittivity and increases the contact area between the CAC particles and air, bringing the value of Z_{in} and Z_{out} closer. Additionally, the surface area plays a role in microwave attenuation. As microwave waves pass through the CAC pores, polarization at the solid-air interface increases the attenuation of the waves. Higher microwave absorption corresponds to lower RL values. A microwave absorber should have an RL value of less than -10 dB, indicating that 90% of the microwave waves are absorbed. The absorbed microwave energy is then dissipated as heat, aiding in the heating of *Sargassum* sp.

CAC is synthesized through various thermal processes, including torrefaction, pyrolysis, gasification, and hydrothermal carbonization. During the production of CAC, it is essential to activate the carbon, either physically or chemically, to enhance its surface area (Gratuito *et al.*, 2008). Chemical activation also allows for the introduction of specific functional groups onto the carbon surface, depending on the activating agent used. Physical activation typically employs steam or CO_2, whereas chemical activation utilizes acids, bases, and salts such as H_3PO_4, NaOH, $ZnCl_2$, $NiCl_2$, and $CuCl_2$ (Gratuito *et al.*, 2008; Cazetta *et al.*, 2011; Saka, 2012). Activation may occur either before or after the thermal processes. In chemical activation, the raw material or the char derived from thermal processes is immersed in a chemical solution for several hours. The subsequent thermal process is performed at temperatures exceeding 300 °C.

This research aimed to investigate the influence of *Sargassum* sp. particle size, temperature, and activated carbon-to-feedstock ratio on the yield of MAP products. The novelty of this research lies in the use of

low pyrolysis temperatures and the effect of the amount of CAC on product yield and calorific value. The researchers selected pyrolysis temperatures from 300-450 °C to determine if MAP is effective yield and bio-oil composition) at these temperatures. Previous researchers conducted pyrolysis at temperatures above 400 °C to ensure the decomposition reaction was complete (Farobie *et al.*, 2022; Amrullah *et al.*, 2024). Additionally, this research chosen particle size range was significantly broad (from 100 to 10 mesh), allowing for the examination of pyrolysis phenomena across various particle sizes.

Furthermore, the bio-oil products obtained were characterized both physically and chemically. This exploratory research serves as a reference for other researchers, enabling them to compare the product yields of MAP *Sargassum* sp. with other materials. The downstream biorefinery of *Sargassum* sp. could support net-zero carbon projects, as *Sargassum* sp. has a greater capacity to absorb CO_2 than the emissions released from its combustion.

MATERIALS AND METHODS

Materials

Sargassum sp. was brought from Mbuluk Beach, Gunungkidul (Yogyakarta, Indonesia). CAC was purchased from CV Alfa Kimia (Yogyakarta, Indonesia).

Sargassum sp. and Coconut Activated Carbon (CAC) Preparation and Characterization

Sargassum sp. was initially sun-dried and oven-dried at 100°C for 4 hours. The dried *Sargassum* sp. was ground into a powder using a grinder and sieved through mesh screens. The powder's characterization of the *Sargassum* sp. included proximate analysis to determine its moisture, volatile matter (Vm), fixed carbon (FC), and ash content.

Similarly, CAC underwent proximate analysis. Before pyrolysis, CAC was oven-dried at 200°C for 2 hours. This procedure ensured that the moisture and Vm in the CAC did not vaporize during pyrolysis.

Microwave-Assisted Pyrolysis (MAP) Process

Before pyrolysis, *Sargassum* sp. was mixed with CAC. The pyrolysis of 50 grams of *Sargassum* sp. was conducted in a Pyrex reactor (10 cm in diameter and height) placed inside a Microwave Electrolux EMM2308X, manufactured by Electrolux Indonesia. The MAP process ran for 20 min with the microwave power set to "High." Pyrolysis was aided by a vacuum pump (¼ pk WIPRO VP-11) to collect the gases formed within the reactor.

The variables in the MAP process were the final pyrolysis temperatures (300, 350, 400, and 450 °C), particle sizes (10-40, 40-70, 70-100, and >100 mesh), and the activated carbon (AC)/feedstock ratios (1:2, 1:1, and 3:2). The experiments involving temperature and particle size variables used a CAC/feedstock ratio of 1:1. The experiments involving the CAC/feedstock ratio used a temperature of 330 °C, as it was the maximum temperature achievable for a CAC/feedstock ratio of 1:2. The schematic of the MAP equipment is presented in Fig. 1. The temperature was recorded every 30 s to create a temperature profile for all particle sizes throughout the pyrolysis.

Bio-oil Characterization

The bio-oil's characteristics were thoroughly analyzed, including density, calorific value, and compound's composition.

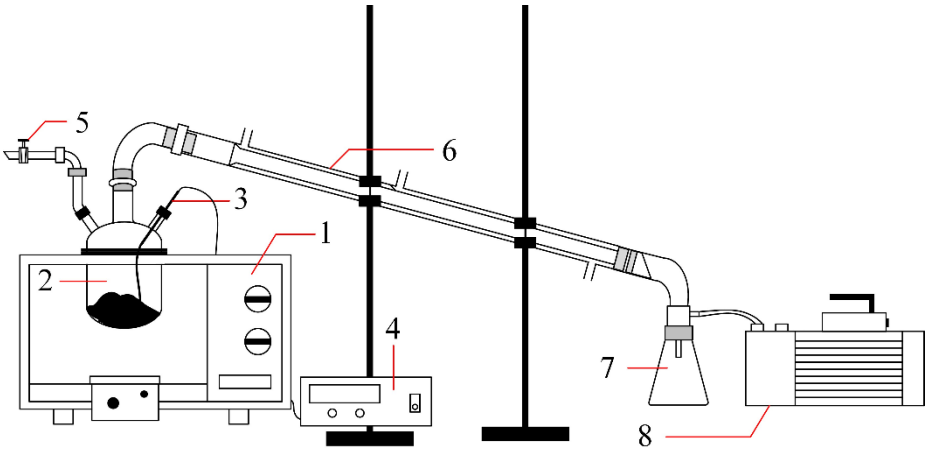

1 Microwave, 2 Pyrex reactor, 3 Thermocouple, 4 Temperature controller, 5 Safety valve, 6 Condenser, 7 Bio-oil collector, 8 Vacuum pump ¼ pk

Fig. 1: Microwave-assisted pyrolysis equipment

The calorific value of the bio-oil was assessed for various CAC/feedstock ratios. The density of the bio-oil samples was measured using a 5 mL Pyrex pycnometer, and the calorific value was determined using a Parr 1341 calorimetric bomb manufactured by Parr Instrument Company, United States.

The organic components of the bio-oil were analyzed using Gas Chromatography-Mass Spectrometry (GC-MS) and Fourier Transform Infrared Spectroscopy (FTIR). The bio-oil analyzed with GC-MS and FTIR was obtained from the MAP process at 350°C.

GC-MS analysis was conducted using a Shimadzu QP 2010S equipped with a Flame Ionization Detector (FID) manufactured by Shimadzu Corporation, Japan. An Rtx-5MS column was utilized, with helium as the carrier gas. The operating parameters included column and injection temperatures of 100°C and 300°C, respectively. The flow rates and velocities were set at 0.44 mL/min, 3.0 mL/min, 24.8 mL/min, and 24.5 cm/s, respectively. The dilution and split factors were 1 (no dilution) and 49, respectively.

Functional groups were identified in the bio-oil using a Thermo Nicolet Avatar 360IR FTIR scanner with potassium bromide (KBR) manufactured by ThermoFisher Scientific, United States.

Data Analysis

The data analysis in this study encompassed the yield of bio-oil, gas, and char across various particle sizes, temperatures, and CAC/feedstock ratios. The yield equations were expressed as follows:

$$\text{char yield } (\%) = \frac{m_C}{m_{B0}}.100\% \quad (1)$$

$$\text{bio} - \text{oil yield } (\%) = \frac{m_L}{m_{B0}}.100\% \quad (2)$$

$$\text{gas yield } (\%) = \frac{m_{B0} - m_C - m_L}{m_{B0}}.100\% \quad (3)$$

$$\text{volatiles yield } (\%) = \text{char yield } (\%) + \text{bio} - \text{oil yield } (\%) \quad (4)$$

Where m_C, m_L, and m_{B0} represented the mass of char, bio-oil, and initial biomass (g). Here, char was considered as the remaining solid, indicating the combination of char with the residual biomass.

RESULTS AND DISCUSSION

Sargassum sp. and Coconut Activated Carbon (CAC) Characterization

The results of the proximate analysis (see Table 1 and Table 2) conducted on *Sargassum* sp. and coconut activated carbon (CAC) have provided significant insights into their characteristics.

Table 1. Proximate analysis of *Sargassum sp.*

Parameters	Results, %
Moisture	14.82
Ash	29.44
Protein	7.78
Total lipid	0.22
Carbohydrate	47.74

*% in weight

The moisture content of 14.82% indicated the total amount of water in *Sargassum* sp. A higher moisture content leads to weaker microwave absorption, particularly at elevated temperatures. The high moisture content in *Sargassum* sp. resulted in microwave absorption being less affected by temperature (Wang *et al.*, 2022). Raw materials with high moisture content require more latent energy from the microwave (Ethaib *et al.*, 2020). During pyrolysis, water vaporizes in the initial phase before primary decomposition, secondary decomposition, cracking, and repolymerization occur (Haeldermans *et al.*, 2019; Kan *et al.*, 2016). Additionally, a higher moisture content is associated with a lower calorific value (Mierzwa-Hersztek *et al.*, 2019).

The ash content of 29.44% indicated the presence of inorganic elements that remain as residual materials after pyrolysis (Kalina *et al.*, 2022). Compared to woody biomass, which typically ranges from 2.6% to 18.3% in ash content (Smołka-Danielowska & Jabłońska, 2022), *Sargassum* sp. exhibited a relatively high ash content. This elevated ash content in *Sargassum* sp. might be attributed to the saline environment in which it grows.

Table 2. Proximate analysis of CAC

Parameters	Results
Moisture	10.530
Ash	6.812
Volatile matter (VM)	6.744
Fixed carbon (FC)	76.014

*% in weight

Approximately half *Sargassum* sp.'s biomass comprised carbohydrates, making it a promising raw material for bio-oil production. Carbohydrates are predominantly carbon-based component, facilitating their thermal conversion into higher-value chemical compounds. However, *Sargassum* sp. also contained significant protein content, leading to the formation of nitrogenous organic compounds during pyrolysis. When bio-oil is used as a fuel, these nitrogen compounds can oxidize, forming nitrogen oxides (NOx).

Similar to *Sargassum* sp., the proximate properties of CAC significantly influenced operational conditions and pyrolysis product yields. High-quality CAC should contain low moisture, volatile matter (Vm) and high fixed carbon (FC) content. To minimize moisture and Vm release from CAC, it was pre-treated by oven-drying at 200°C for 2 hours before use. In this experiment, CAC exhibited high FC and ash content with relatively low moisture and Vm content.

Temperature Profiles during MAP Process

The temperature profile was designed to observe heating rate trends across various particle sizes and to identify distinct phases during pyrolysis. The pyrolysis process was

notably influenced by its heating rate, a factor intricately linked to the particle size within the MAP (See Fig. 2). Particle size played a pivotal role in determining the heating rate within the MAP process, with smaller particles exhibiting a higher heating rate owing to their larger surface area, facilitating enhanced convection heat transfer. However, this trend was not observed for particle sizes exceeding 100 mesh. Remarkably diminutive particle sizes lead to increased bulk density, subsequently impacting the thermal diffusivity of the material within the reactor. Consequently, the heat transfer process is attenuated with escalating bulk density, culminating in a slower heat transfer rate (Presley and Christensen, 2010).

For instance, temperature attainment within the range of 10-40 mesh occurred in 6 min and 40 s, while for 40-70 mesh, it took 7 min and 15 s. Similarly, temperatures were reached in 7 min and 30 s for 70-100 mesh and 7 min and 46 s for particle sizes exceeding 100 mesh.

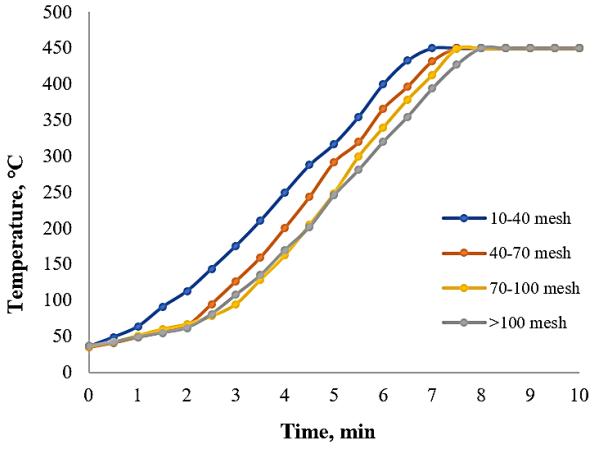

Fig. 2: Temperature profile in MAP process up to 10 min

The temperature profile data revealed three distinct regions characterized by varying slopes. The initial region lasted from 0 to 3 min, during which temperatures ranged between 35°C and 81°C. Subsequently, the second region extended from 3 to 8 min period, exhibiting temperatures ranging from 81°C to 450°C. Beyond the 8-min, a third region emerged, maintaining a constant temperature of 450°C.

Each of these regions corresponded to specific thermal phenomena. The first region corresponded to the evaporation of water and the devolatilization of volatile matter (VM). The second region signified a phase of intensified devolatilization, decomposition, and cracking processes. Finally, the third region denoted a stable state wherein further decomposition and cracking processes persisted (Zhang *et al.* 2017). A study on the decomposition of *Sargassum plagiophyllum* was conducted by Amrullah *et al.* (2024) using thermogravimetric analysis (TGA). The conventional pyrolysis process revealed three distinct mass loss regions: below 278 °C, between 278 °C and 398 °C, and above 398 °C. The most significant mass loss was attributed to the devolatilization and decomposition of large molecules, such as carbohydrates and proteins. Even at temperatures above 600 °C, S. *plagiophyllum* continued to undergo decomposition of inorganic substances. The difference in the temperature range observed in this study compared to Amrullah *et al.* (2024) was attributed to the different types of pyrolysis processes used. Amrullah *et al.* (2024) conducted their research using slow pyrolysis.

Effect of Particle Size and Temperature on MAP Products Yields

In the experiments conducted at all final pyrolysis temperatures (300, 350, 400, 450 °C) , particles within the size range of 40–70 mesh yielded the highest yield of volatiles and bio-oil (See Fig. 3 and Fig. 4). In contrast, particle size >100 mesh resulted in the lowest volatiles yield and bio-oil. At temperatures

300 to 450 °C, the highest gas yield was obtained from 70-100 mesh particle sizes (See Fig. 6).

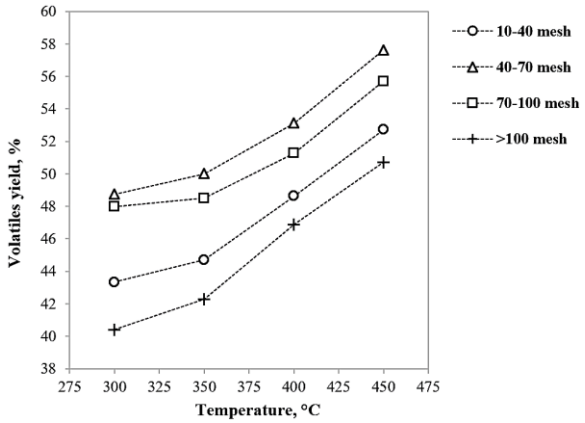

Fig. 3: Volatiles yield at different final MAP temperature and particle sizes

Generally, when bio-oil is desired as the main product, pyrolysis is conducted at temperatures >425°C (Yang *et al.*, 2019). However, in this experiment, from 300 to 450 °C, the gas yield was consistently higher compared to the bio-oil yield. With an increase in pyrolysis temperature, the process tends towards gasification.

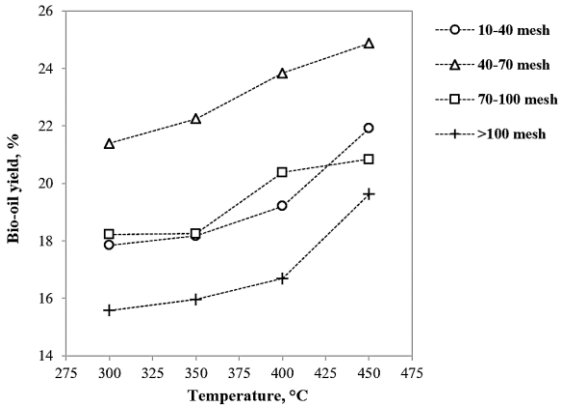

Fig. 4: Bio-oil yield at different final MAP temperature and particle sizes

The highest yield for gas (34.870%) was achieved at a temperature of 450 °C at the particle size of 70–100 mesh, while the lowest gas yield (24.822%) was achieved at a temperature of 300 °C at a particle size of >100 mesh. In contrast to gas, the highest char yield was obtained from a particle size >100 mesh and at a pyrolysis temperature of 300°C (see Fig. 5). Compared to conventional pyrolysis, MAP requires lower temperatures and shorter pyrolysis time to initiate biomass decomposition and cracking. As obtained from direct observation, at 80°C, water began to evaporate, and volatiles began to form. Bio-oil started to form in the 2nd min of operation.

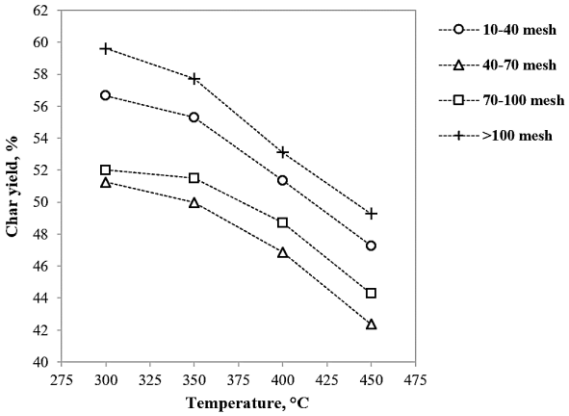

Fig. 5: Char yield at different final MAP temperature and particle sizes

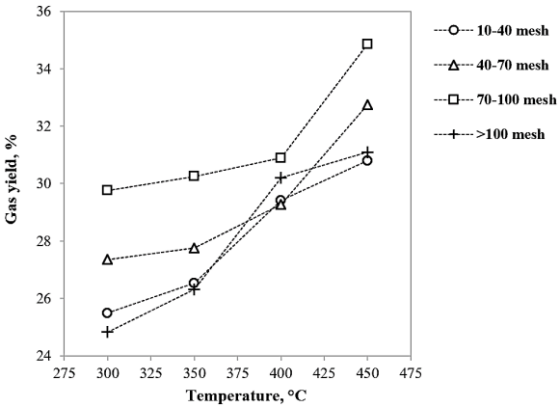

Fig. 6: Gas yield at different final MAP temperature

For the 40–70 mesh particle size, at the final pyrolysis temperature of 300 °C, the yield of volatiles was 48.746%, comprised of 21.388% bio-oil and 27.358% gas. At 350 °C,

the yield of volatiles was 50.010%, comprised of 22.250% bio-oil and 27.760% gas. At 400 °C, the yield of volatiles was 53.120%, comprised of 23.844% bio-oil and 29.276% gas. The highest volatile yield (57.636%) was obtained at a final temperature of 450 °C, with bio-oil and gas constituting 24.878% and 32.758%, respectively. While, the lowest volatile yield (43.336%) was obtained for particle sizes >100 mesh at a temperature of 300 °C, with 15.576% bio-oil and 24.822% gas.

Particle size is closely related to a particle's ability to directly absorb microwave radiation, and the heat energy dissipated by CAC. The particle's ability to absorb microwaves is connected to the theory of penetration depth, in which each particle has a different penetration depth (δ). Penetration depth is defined as the distance from the material's surface to a certain distance (in a sphere, the distance is defined as a radius) at which microwaves power decreases to 1/e (approximately 37%) of its surface level. This parameter quantifies how effectively microwave can penetrate a material (Tripathi *et al.*, 2015).

When the particle size is very small, the particles quickly absorb microwaves, leading to rapid and uniform particle heating. In contrast, larger particle sizes provide a greater volume for wave absorption, resulting in more effective particle heating and higher particle temperatures. However, if the δ value is significantly smaller than the particle radius (r), heating takes longer, and there is temperature distribution within the particle (Jie *et al.*, 2022). In addition, the presence of CAC is highly beneficial for heating *Sargassum* sp. because CAC is an effective microwave absorber (Yusuf *et al.*, 2022).

In this study, the particle size of 40-70 mesh was found to be the optimum size where microwave and heat can effectively induce particle reactions. Particle sizes that are not too small initiate the heating of nearby particles because they provide a larger heat volume. Conversely, particle size >100 mesh resulted in lower volatile yields. This was also related to the high bulk density of the *Sargassum* sp. and CAC mixture, which prolonged microwave induction to the center of the reactor. Smaller particles resulted in a higher bulk density, thereby leading to a reduction in the thermal conductivity of *Sargassum* sp. (Presley & Christensen, 2010). The MAP process used a Pyrex reactor with an outside diameter of 10 cm, resulting in temperature distribution within the reactor (from r = 5 cm to the center of the reactor).

Many other researchers investigated the impact of particle size on MAP bio-oil and gas yields (Flicler *et al.*, 2023; Huang *et al.*, 2018; Shang *et al.*, 2015). These studies demonstrated an optimum particle size that yielded the highest volatile yields. Flicler *et al.* (2023) varied the particle size of agricultural waste (wheat bran, straw, sawdust, rice husk, and nutshell) from 140–2000 µm, and the optimum volatile yield was obtained at a size of 800 µm. For sizes ranging from 1000–2000 µm, larger sizes resulted in decreased bio-oil and gas yields, with increased char yield. In the pyrolysis of corn stover conducted by Huang *et al.* (2018), various sizes were tested (5, 10, 40, 60, and 100 mesh), and the highest bio-oil yield was observed at 5 mesh, while the highest gas yield was at 60 mesh. The highest yield of bio-oil in sawdust pyrolysis performed by Shang *et al.* (2015) was obtained from sizes 0.5–0.8 mm (size distribution: 0.25-0.5; 0.5-0.8; >0.8 mm), but volatile yields increased as particle size increased.

Several previous researchers studied the effect of the MAP temperature on pyrolysis

product yields (Wang *et al.*, 2021; Zhou *et al.*, 2021; Wallace *et al.*, 2019). These research results indicated that increasing the MAP temperature led to an increase in volatile yield. Wang *et al.* (2021) varied the pyrolysis temperature at 400, 500, and 600°C. The highest bio-oil yield was achieved at 500°C, but the highest yield of volatiles was achieved at 600°C. This trend was similar to Zhou *et al.* (2021), who varied the pyrolysis temperature at 540, 560, 620, and 750°C. The research result show that the highest bio-oil yield was achieved at 560°C, but the yield of volatiles continued to increase with an increase in temperature. Similarly, in the study by Wallace *et al.* (2019), as the heating rate and temperature increased, the biomass decomposition rate was higher, leading to the formation of liquid and gas and a decrease in char.

Effect of CAC/Feedstock Ratio on MAP Product Yields

This research employed various CAC/feedstock ratios of 1:2, 1:1, and 3:2 (See Fig. 7). The research results showed that AC played a significant role in forming volatiles. A higher CAC/feedstock ratio led to a greater bio-oil yield. This was because CAC assist in heating *Sargassum* sp. by acting as an excellent microwave absorber due to its high dielectric tangent loss (tanδ) (Vignesh *et al.*, 2022; Ethaib *et al.*, 2020). A high tanδ value caused increased heat dissipation (Chuayjumnong *et al.*, 2020).

CAC not only enhanced volatile yield but also increased the maximum MAP temperature. Without AC, the pyrolysis temperature could not reach the desired level. As stated before, a higher heating rate yielded higher volatiles (Mokhtar *et al.*, 2018). The highest volatiles yield (53.706%) was achieved with a CAC/feedstock ratio of 3:2. The bio-oil yield increased with the addition of CAC, while the gas yield decreased. In this context, it could be concluded that CAC assisted in the formation of condensable gas. However, the quantity of CAC did not have a linear relationship with the calorific value of the bio-oil (see Table 4). A CAC/feedstock ratio of 1:2 resulted in a maximum pyrolysis temperature of 330°C. Therefore, this research used a maximum pyrolysis temperature of 330°C to examine the effect of the CAC/feedstock ratio. Once the temperature reached a steady state, it was maintained for a total pyrolysis time of 20 min.

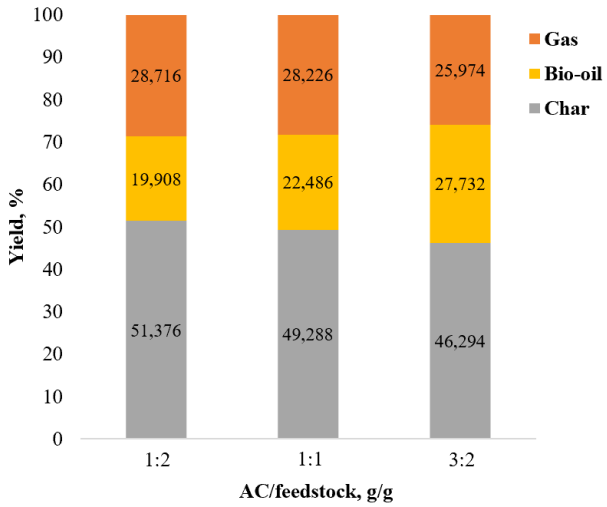

Fig. 7: MAP products yield at different CAC/feedstock ratio

AC influenced the heating rate of the MAP process by enhancing microwave absorption (Shi *et al.*, 2023; Khelfa *et al.*, 2020; Mokhtar *et al.*, 2018). In the research conducted by Shi *et al.* (2023), the CAC amount was directly proportional to the heating rate. According to Khelfa *et al.* (2020), 10% AC increased the bio-oil yield and help achieve a final pyrolysis temperature of 505 ± 2 °C. . Similarly, as in Khelfa *et al.* (2020), the study by Mokhtar *et al.* (2018) also demonstrated that AC could increase bio-oil

yield and decrease char yield. Mokhtar *et al.* (2018) varied the amount of CAC by 5%, 10%, and 20%. A 20% CAC increase in the maximum pyrolysis temperature and heating rate was shown. As the amount of CAC increased, more gas was generated (Mokhtar *et al.*, 2018; Ellabban *et al.*, 2014). This occurred because, at high heating rates, secondary cracking reactions occurred more frequently. However, at 10% CAC, the generated gas had the highest Lower Heating Value (LHV) due to its higher H_2 content.

Char and Bio-oil Characterization

The characterization of char included proximate analysis (see Table 3). In this study, char comprised the remaining solid, a combination of biomass and char. The char samples were obtained from a study conducted at 450°C, utilizing particles sized between 40-70 mesh, with an activated carbon (AC) to feedstock ratio of 1:1.

Table 3. Proximate analysis of *Sargassum* sp.

Parameters	Results, %
Moisture	2,00
Ash	28,45
Protein	5,38
Total lipid	0,12
Carbohydrate	64,05

*% in weight

The study results demonstrated a reduction in moisture, ash, protein, and total lipid levels. This phenomenon suggested that during the pyrolysis process, nearly all water was evaporated, accompanied by the decomposition of proteins and total lipids. The decline in ash content was likely attributable to the release of alkali and alkaline earth metals (AAEMs) into the gas or bio-oil products (Jendoubi *et al.*, 2011). Notably, the carbohydrate content in *Sargassum* sp. remained unchanged. The observed increase in carbohydrates in the proximate analysis of char was attributed to the presence of activated carbon, which, upon analysis, might be classified as carbohydrates. It was noteworthy that activated carbon inherently contained a trace amount of ash.

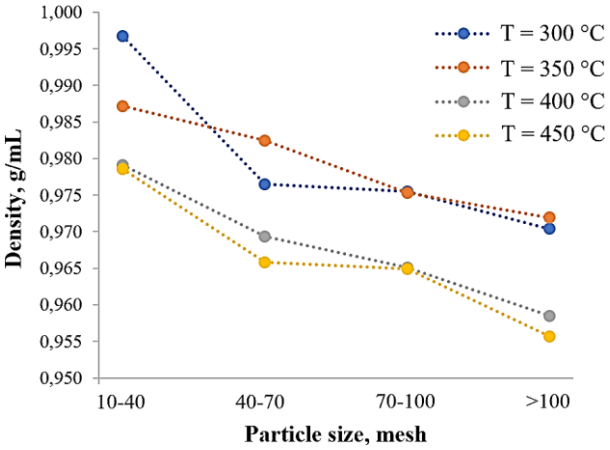

Fig. 8: Bio-oil density at different final temperature and particle size

This study's measurable bio-oil density varied, ranging from 0.9557 to 0.9968 g/mL (See Fig. 8). A density close to 1 indicated that the majority of bio-oil was water. The trend showed an inverse relationship between density and temperature. This was because, the hydrocarbon fraction in bio-oil increased at higher temperatures due to biomass decomposition into volatiles. The highest bio-oil density was achieved at a 10-40 mesh particle size and a final temperature of 300°C. This indicated that at this temperature and particle size, the pyrolysis process was only in the initial stage of water evaporation (Haeldermans *et al.*, 2019). The lowest bio-oil density was obtained at a particle size >100 mesh with an operating temperature of 450°C.

CV testing was conducted on bio-oil samples produced through pyrolysis with

varying CAC/feedstock ratios of 1:2, 1:1, and 3:2 at 330°C (see Table 4). The results showed that a 1:1 CAC/feedstock ratio produced the highest CV value. At 330°C, the formation of hydrocarbon components in bio-oil was not yet optimal, resulting in a relatively low CV.

At this temperature, the primary process was water evaporation, leading to a higher water content in the bio-oil product. Consequently, a higher water content tended to decrease the CV value. It is important to note that these CV values do not meet the standards required for industrial purposes and transportation fuels, similar to conventional crude oil and petrol. Therefore, further advanced upgrading process is needed to align the pyrolysis bio-oil's properties with industrial and transportation standards.

The examination of bio-oil constituents alongside their functional groups was carried out employing GC-MS and FTIR. This investigation was conducted on bio-oil subjected to pyrolysis at 350°C, indicating an incomplete decomposition state. The resulting GC data of the bio-oil are delineated in Table 5. Subsequently, the identified compounds are presented in Table 6.

The GC-MS analysis results revealed that the predominant components of the bio-oil were 3,5-Cyclocholestan-19-al, 6-hydroxy-, (6.beta.)- (44.02 %TIC) and butanoic acid (37.42 %TIC). The compound 3,5-Cyclocholestan-19-al, 6-hydroxy-, (6.beta.)- (See Fig. 9b) is a derivative of sterol (lipid) based on its aliphatic cyclic structure. This indicated that at 350°C, sterols had not undergone complete decomposition.

Table 4. The calorific value of bio-oil from different CAC/feedstock ratios

Sample	T, °C	CAC/ feedstock	CV, cal/g
1	330	1:2	124.8565
2	330	1:1	134.2530
3	330	3:2	83.3480

Table 5. GC result of bio-oil

Peak	Retention time, min	%TIC
1	1.767	37.42
2	17.178	44.02
3	19.366	18.56

%TIC: Total Ion Chromatogram

Table 6. MS result of bio-oil

Retention time, min	Compound	Group	Chemical Formula	Relative mass, g mol^{-1}	Boiling point, °C
1.767	Butanoic acid	Aliphatic, carboxylic acid	$C_4H_8O_2$	88	163,5
17.178	3,5-Cyclocholestan-19-al, 6-hydroxy-, (6.beta.)-	Aliphatic, aliphatic cyclic, aldehyde, hydroxide	$C_{27}H_{44}O_2$	400	>200
19.366	3-Chloro-2-(1-pyrrolidinocarbonyl) thianaphthene	Halide, aromatic (benzothiophene), ketone, aliphatic cyclic (pyrrolidine)	$C_{13}H_{12}ClNOS$	265	243,7
	4'-Hydroxydihydro-2-stilbazole	Aromatic, hydroxide	$C_{13}H_{13}NO$	199	327.5

Butanoic acid (See Fig. 9a) is produced from the decomposition of cellulose. During pyrolysis, cellulose degrades at temperatures between 315–400°C (Mashuni and Jahiding, 2021). Butanoic acid formation can also originate from levoglucosan, a sugar produced from cellulose decomposition.

Aromatic compounds were formed at a high retention time (19.366 min), (See Fig. 9c and Fig. 9d). Theoretically, aromatic compounds are formed from lignin decomposition at higher pyrolysis temperatures, typically between 400–600°C, or protein decomposition (McGrath *et al.*, 2003; Farobie *et al.*, 2022). However, in this study, aromatic compounds were already detected at 350°C.

The functional groups present in the bio-oil were identified utilizing FTIR spectroscopy (See Fig. 10). In general, the findings from FTIR corroborated those from GC-MS analysis, indicating the presence of its main functional groups, namely carboxylic acid, hydroxyl, amide, amine, aromatic, and aliphatic groups.

The FTIR spectrum revealed a prominent and broad peak centered around 3450 cm^{-1}, indicating the presence of carboxylic acid (-C(=O)OH) and hydroxyl (-OH) groups. A medium and sharp peak manifested the carbonyl (C=O) stretching vibration at approximately 1700 cm^{-1}. These carbonyl groups were attributed to the aldehyde moiety in the compound 3,5-Cyclocholestan-19-al, 6-hydroxy-, (6.beta.)-, the amide functionality in the compound 3-Chloro-2-(1-pyrrolidinocarbonyl) thianaphthene, and the carboxylate group in butanoic acid.

The study on the pyrolysis of *Sargassum* sp. conducted by Farobie *et al.* (2022) revealed that low molecular weight carboxylic acids (propanoic acid and acetic acid) were found in significant amounts in the bio-oil, while butanoic acid was present in lesser quantities. However, the overall concentration of carboxylic acids decreased with increasing pyrolysis temperatures.

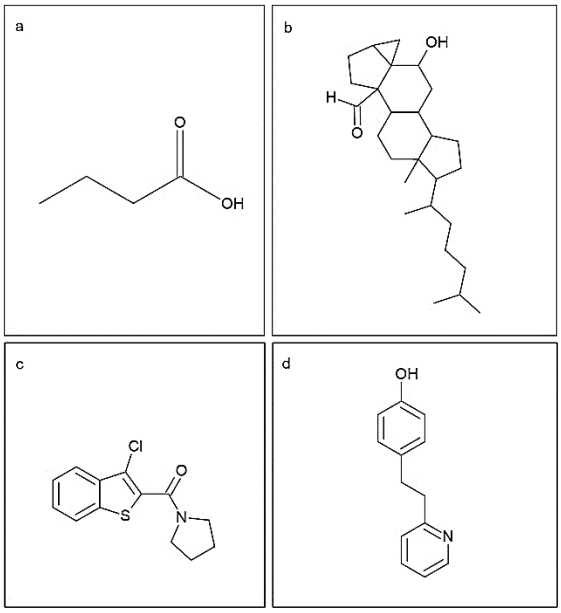

Fig. 9. : Organic compounds found in bio-oil: (a) butanoic acid; (b) 3,5-Cyclocholestan-19-al, 6-hydroxy-, (6.beta.)-; (c) 3-Chloro-2-(1-pyrrolidinocarbonyl) thianaphthene; (d) 4'-Hydroxydihydro-2-stilbazole

The presence of amide (-C(=O)N-) and amine (-N-) groups was discernible in the spectral region spanning 3300–3400 cm^{-1}, which overlaps with the absorption bands of hydroxyl and carboxylate groups. Additionally, the weak-medium and broad peaks in the 2100–2200 cm^{-1} spectral range suggested the presence of C-N bonds. Twin weak peaks observed at approximately 1400 and 1500 cm^{-1} evidenced aromatic functionalities.

The peaks corresponding to aliphatic groups were less prominent here (typically around a wavelength of approximately 3000 cm^{-1}). This could be due to their shifting caused by the strong presence of carboxylic acid and hydroxyl groups and the relatively low dominance of aliphatic groups in the bio-

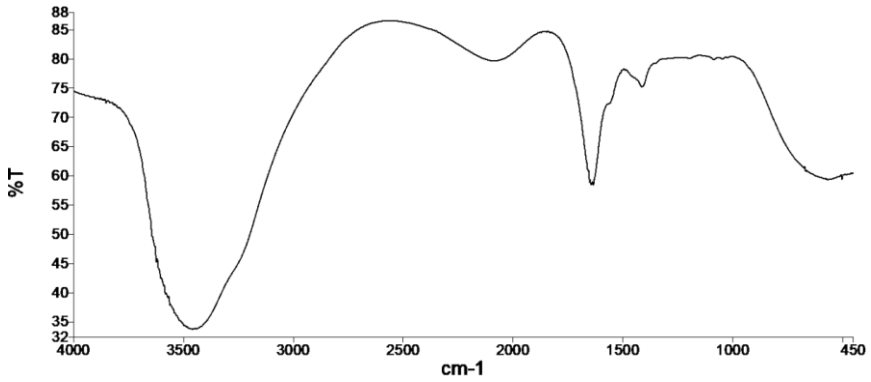

Fig. 10. FTIR result of bio-oil

oil compared to other compounds possessing stronger intermolecular interactions.

Generally, the formed bio-oil holds significant potential as a raw material for the chemical industry. Among the three other compounds present in the bio-oil, butanoic acid exhibits the greatest utilization potential. Butanoic acid can be employed as a fuel; however, its economic value is considered low. Instead, its ester derivatives serve as safe food preservatives, positioning butanoic acid as a valuable building block (Karimi & Vahabzadeh, 2014). Conversely, compounds other than butanoic acid are better suited for academic purposes.

Butanoic acid can be readily separated from the other compounds via distillation, leveraging the principle of differing volatilities among substances. Its considerably lower boiling point distinguishes it from the others. Due to its relatively high boiling point, distillation towers are operated under vacuum conditions to minimize operational costs.

CONCLUSIONS

Particle size, temperature, and CAC/feedstock ratio significantly influenced the yield of bio-oil, gas, and char. The highest volatile yield (67.636%) was achieved with *Sargassum* sp. particles sized 40-70 mesh at an operating temperature of 450 °C, with bio-oil and gas yields of 26.878% and 40.758%, respectively. Meanwhile, the lowest volatile yield (42.398%) was obtained with *Sargassum* sp. particles >100 mesh under operating conditions of 300°C, resulting in bio-oil and gas yields of 17.576% and 24.822%, respectively. Particle size affected the heating rate of MAP, with smaller particle sizes resulting in lower heating rates due to their high bulk density. The addition of CAC increased the maximum MAP temperature and enhanced volatiles and bio-oil yields. At a temperature of 330°C, a CAC/feedstock ratio 1:1 yielded the highest calorific value. The density of bio-oil varied from 0.9557 to 0.9968 g/mL.

For bio-oil, the maximum calorific value from pyrolysis at 330°C was very low (134.2530 cal/g), suggesting that further advanced upgrading is required to meet industrial or transportation fuel standards. From GC-MS analysis, bio-oil contained butanoate acid, which holds significant potential for utilization as a safe food preservative and building block. Other identified compounds, such as 3,5-Cyclocholestan-19-al, 6-hydroxy-, (6.beta.); 3-Chloro – 2 - (1 - pyrrolidinocarbonyl) thiana-

phthene; and 4'-Hydroxydihydro-2-stilbazole, may find application in academic research endeavors. FTIR analysis identified peaks of aromatic (1400 and 1500 cm^{-1}), carbonyl (1700 cm^{-1}), C-N bonds (2100-2200 cm^{-1}), amide and amine (3300-3400 cm^{-1}), and hydroxyl and carboxylic acid (3450 cm^{-1}).

These findings underscored the efficacy of MAP in achieving high volatile yields at relatively moderate temperatures compared to conventional methods. Moreover, butanoic acid's presence in the bio-oil highlighted its potential as a valuable resource for safe food preservation and chemical synthesis. However, detecting of sterol derivatives and complex N-aromatic compounds suggested incomplete decomposition at 350 °C.

REFERENCES

Ahmed, A.S., Uliu, C.H., Hossain, A.B.M.S., Alrudayni, H.A., and Kapilan, N., 2023. "Microwave assisted pyrolysis of Moringa seed and Karanja for bio-oil production." *Int. J. Renew. Energy Res. 13*, 14-24.

Ali-Ahmad, S., Karbassi, A. R., Ibrahim, G., and Slim, K., 2020. "Pyrolysis optimization of Mediterranean microalgae for bio-oil production purpose." *Int. J. Env. Sci. and Technol*. 17, 4281-4290.

Amrullah, A., Fatriasari, W., Sholeha, N. A., Hartulistiyoso, E., & Farobie, O., 2024. "Sustainable biofuel production from brown and green macroalgae through the pyrolysis." *J. Renew. Mater*. *12*(6), 1087-1102

Atwater, J.E. and Wheeler, Jr R.R., 2004. "Temperature dependent complex permittivities of graphitized carbon blacks at microwave frequencies between 0.2 and 26 GHz." *J. Mater. Sci. 39*, 151–7.

Cazetta, A. L., Vargas, A. M. M., Nogami, E. M., Kunita, M. H., Guilherme, M. R., Martins, A. C., Silva, T. L., Moraes, J. C. G., and Almeida, V. C., 2011. "NaOH-activated carbon of high surface area produced from coconut shell: Kinetics and equilibrium studies from methylene blue adsorption." *Chem. Eng. J. 174*, 117-125.

Cheng, J. B., Shi, H. G., Cao, M., Wang, T., Zhao, H. B., and Wang, Y. Z., 2020. "Porous carbon materials for microwave absorption." *Mater. Adv*. *1*, 2631-2645.

Chitraningrum, N., Marlina, R., Arundina, R. Y., Suryani Togatorop, E. R., Sulistyaningsih, Arisesa, H., Budiman, I., Daud, P., and Hamzah, M., 2022. "Microwave absorption properties of porous activated carbon-based palm oil empty fruit bunch." *AIP Adv*. 12, 35083–35093.

Chuayjumnong, S., Karrila, S., Jumrat, S., and Pianroj, Y., 2020. "Activated carbon and palm oil fuel ash as microwave absorbers for microwave-assisted pyrolysis of oil palm shell waste." *RSC Adv. 10*, 32058-32068.

Du, Z., Li, Y., Wang, X., Wan, Y., Chen, Q., Wang, C., Lin, X., Liu, Y., Chen, P., and Ruan, R., 2011. "Microwave-assisted pyrolysis of microalgae for biofuel production." *Bioresour. Technol. 102*, 4890–4896.

Ellabban, O., Abu-Rub, H. and Blaabjerg, F., 2014. "Renewable energy resources: Current status, future prospects and their enabling technology." *Renew. Sustain. Energy Rev*. *39*, 748-764.

Ethaib S., Omar R., Kamal S. M. M., Biak, D. R. A., and Zubaidi, S. L., 2020. "Microwave-Assisted pyrolysis of biomass waste: A mini review." *Processes 8*, 1–17.

Farobie, O., Amrullah, A., Syaftika, N., Anis, L. A., and Hartulistiyoso, E., 2022. "In-depth study of bio-oil and biochar production

from macroalgae *Sargassum* sp. *via* slow pyrolysis." *RSC Adv. 12*, 9567-9578.

Feng, Y. and Meier, D., 2017. "Supercritical carbon dioxide extraction of fast pyrolysis oil from softwood." *J. Supercrit. Fluid 128*, 6-17.

Fricler, V.Y., Nyashina, G.S., Vershinina, K.Yu., Vinogrodskiy, K.V., Shvets, A.S., and Strizhak, P.A. "Microwave pyrolysis of agricultural waste: Influence of catalysts, absorbers, particle size and blending components." *J. Anal. Appl. Pyrol. 171*, 105962.

Ghodke, P. K., Ramanjaneylu, B., and Kumar, S., 2023. "Stabilization of bio-oil derived from macroalgae biomass using reactive chromatography." *Biomass Convers. Bioref. 13*, 5261–5272.

Gratuito, M. K. B., Panyathanmaporn, T., Chumnanklang, R.-A., Sirinuntawittaya, N., and Dutta, A., 2008. "Production of activated carbon from coconut shell: Optimization using response surface methodology." *Bioresour. Technol. 99*, 2887-4895.

Gupta, G. K. and Mondal, M. K., 2022. Chapter 14 – Pyrolysis: an alternative approach for utilization of biomass into bioenergy generation. Gurunathan, B., Sahadevan, R., and Zakaria, Z.A., eds., *Biofuels and Bioenergy*. Elsevier, Amsterdam.

Haeldermans, T., Claesen, J., Maggen, J., Carleer, R., Yperman, J., Adriaensens, P., Samyn, P., Vandamme, D., Cuypers, A., Vanreppelen, K., and Schreurs, S., 2018. "Microwave assisted pyrolysis of MDF: the influence of microwave power and microwave absorbers on the pyrolysis process and biochar characteristics. A comparison with conventional pyrolysis." *J. Anal. Appl. Pyrol.* 138, 218-230.

Huang, Y-F., Kuan, W-H., and Chang, C-Y., 2018. "Effects of particle size, pretreatment, and catalysis on microwave pyrolysis of corn stover." *Energy. 143*, 696-703.

Jamilatun, S., Budhijanto, Rochmadi, Yuliestyan, A., and Budiman, A. 2019. "Valuable chemicals derived from pyrolysis liquid products of *Spirulina platensis* residue." *Indones. J. Chem. 19*, 703–711.

Jendoubi, N., Broust, F., Commandre, J. M., Mauviel, G., Sardin, M. and Lédé, J., 2011. "Inorganic distribution in bio-oils and char produced by biomass fast pyrolysis: The key role of aerosols" *J. Anal. Appl. Pyrol. 92*, 59-67.

Jesus, M. S. de, Martinez, C. L. M., Costa, L. J., Pereira, E. G., and Carneiro, A. C. O. de., 2020. "Thermal conversion of biomass: a comparative review of different pyrolysis processes." *Revista Ciência da Madeira - RCM*, *11*. 12–22.

Jie, X., Chen, R., Biddle, T., Slocombe, D. R., Dilworth, J. R., Xiao, T., and Edwards, P. P., 2022. "Size-dependent microwave heating and catalytic activity of fine iron particles in the deep dehydrogenation of hexadecane." *Chem. Mater. 34*, 4682-4693.

Kalina, M., Sovova, S., Svec, J., Trudicova, M., Hajzler, J., Kubikova, L., and Enev, V., 2022. "The effect of pyrolysis temperature and the source biomass on the properties of biochar produced for the agronomical applications as the soil conditioner." *Materials 15*, 2–13.

Kan, T., Strezov, V., and Evans, T.J., 2016. "Lignocellulosic biomass pyrolysis: A review of product properties and effects of pyrolysis parameters." *Renew. Sustain. Energy Rev. 57*, 1126–1140.

Karimi, G. and Vahabzadeh, M., 2014. Butyric Acid. Wexler, P., ed., Encyclopedia of

Toxicology. Elsevier. Amsterdam. 597-601.

Khelfa, A., Rodrigues, F. A., Koubaa, M., and Vorobiev, E., 2020. "Microwave-assisted pyrolysis of pine wood sawdust mixed with activated carbon for bio-oil and bio-char production." *Processes 8*, 1–12.

Lin, H., Zhu, H., Guo, H., and Yu L. 2008. "Microwave-absorbing properties of Co-filled carbon nanotubes." *Mater. Res. Bull. 43*, 2697–2702.

Mashuni and Jahiding, M., 2021. The Biomass Waste Pyrolysis for Biopesticide Application. Bartoli, M., ed., *Recent Perspectives in Pyrolysis Research* Intechopen, London.

Marland, S., Merchant, A., and Rowson, N., 2001. "Dielectric properties of coal." *Fuel 80*, 1839–49.

McGrath, T. E., Chan, W. G., and Hajaligol, M. R., 2003. "Low temperature mechanism for the formation of polycyclic aromatic hydrocarbons from the pyrolysis of cellulose." *J. Anal. Appl. Pyrol. 66*, 51-70.

Mierzwa-Hersztek, M., Gondek, K., Jewiarz, M., and Dziedzic, K., 2019. "Assessment of energy parameters of biomass and biochars, leachability of heavy metals and phytotoxicity of their ashes." *J. Mater. Cycles Waste Manag. 21*, 786–800.

Mokhtar, M. N., and Ethaib, S., 2018. "Effects of Microwave Absorbers on The Products of Microwave Pyrolysis of Oily Sludge." *J. Eng. Sci. Technol., 13 (10),* 3313 - 3330.

Mushtaq, F., Mat, R., and Nasir, F., 2014. "A review on microwave assisted pyrolysis of coal and biomass for fuel production." *Renew. Sustain. Energy Rev. 39*, 555–574.

Nam, H., Choi, J., and Capareda, S. C., 2016. "Comparative study of vacuum and fractional distillation using pyrolytic microalgae (*Nannochloropsis oculata*) bio-oil." *Algal Res. 17*, 87–96.

Omar, R., Idris, A., Yunus, R., Khalid, K., and Aida Isma, M.I., 2011. "Characterization of empty fruit bunch for microwave-assisted pyrolysis." *Fuel 90*, 1536–44.

Presley, M.A. and Christensen, P.R., 2010. "Thermal conductivity measurements of particulate materials: 4. Effect of bulk density for granular particles." *J. Geophys. Res. 115*, E07003.

Pourkarimi, S., Hallajisani, A., Alizadehdakhel, A., and Nouralishahi, A., 2019. "Biofuel production through micro- and macroalgae pyrolysis – A review of pyrolysis methods and process parameters." *J. Anal. Appl. Pyrol. 142*, 1–19.

Pradana, Y. S., Sudibyo, H., Suyono, E. A., Indarto, and Budiman, A. 2017., "Oil algae extraction of selected microalgae species grown in monoculture and mixed cultures for biodiesel production." *Energy Procedia. 105*, 277–282.

Saka, C., 2012. "BET, TG-DTG, FT-IR, SEM, iodine number analysis and preparation of activated carbon from corn shell by chemical activation with $ZnCl_2$". *J. Anal. Appl. Pyrol. 95*, 21-24.

Salosso, Y., 2019. "Nutrient and alginate content of macroalgae *Sargassum* sp. from Kupang bay waters, East Nusa Tenggara, Indonesia." *AACL Bioflux. 12*, 2130–2136.

Shang, H., Lu, R-R., Shang, L., and Zhang, W-H., 2015. "Effect of additives on the microwave-assisted pyrolysis of sawdust." *Fuel Process. Technol. 131*, 167-174.

Shi, C., Shi, H., Li, H., Liu, H., Mostafa, E., Zhao, W., and Zhang, Y., 2023. "Efficient heating of activated carbon in microwave field." *J. Carbon Res. 9*, 48.

Smołka-Danielowska, D., and Jabłońska, M., 2022. "Chemical and mineral

composition of ashes from wood biomass combustion in domestic wood-fired furnaces." *Int. J. Environ. Sci. Technol. 19*, 5359–5372.

Sodiq, A. Q., and Arisandi, A., 2020. "Identifikasi dan Kelimpahan Makroalga di Pantai Selatan Gunungkidul." *Juvenil: Jurnal Ilmiah Kelautan dan Perikanan*, *1*, 325–330.

Torgovnikov GI. 1993. Dielectric properties of wood and wood-based materials. Springer-Verlag, Berlin.

Tripathi, M., Sahu, J. N., Ganesan, P., and Dey, T. K., 2015. "Effect of temperature on dielectric properties and penetration depth of oil palm shell (OPS) and OPS char synthesized by microwave pyrolysis of OPS." *Fuel 153*, 257–266.

Vignesh, N. S., Soosai, M. R., Chia, W. Y., Wahid, S. N., Varalakshmi, P., Moorthy, I. M. G., Ashokkumar, B., Arumugasamy, S. K., Selvarajoo, A., and Chew, K. W., 2022. "Microwave-assisted pyrolysis for carbon catalyst, nanomaterials and biofuel production." *Fuel 313*, 123023.

Wallace, C. A., Afzal, M. T., and Saha, G. C., 2019. "Effect of feedstock and microwave pyrolysis temperature on physio-chemical and nano-scale mechanical properties of biochar." *Biores. Bioprocess*, *6* (33), 1-11.

Wang, D., Li, X., Hao, X., Lv, J., and Chen, X., 2022. "The effects of moisture and temperature on the microwave absorption power of poplar wood." *Forests 13*, 309.

Wang, H., Meyer, P. A., Santosa, D. M., Zhu, C., Olarte, M. v., Jones, S. B., and Zacher, A. H., 2021. "Performance and techno-economic evaluations of co-processing residual heavy fraction in bio-oil hydrotreating." *Catal. Today 365*, 357–364.

Wang, S-W., Li, D-X., Ruan, W-B., Jin, C-L., and Farahani, M.R., 2018. "A techno-economic review of biomass gasification for production of chemicals." *Energy Sources B: Econ. Plan. Policy. 13*, 351-356.

Wang, X., Li, C., Chen, M., and Wang, J., 2021. "Microwave-assisted pyrolysis of seaweed biomass for aromatics-containing bio-oil production." *E3S Web Conf. 261*, 02045.

Wibowo, W. A., Cahyono, R. B., Rochmadi, R., and Budiman, A., 2023. "Kinetics of in-situ catalytic pyrolysis of rice husk pellets using a multi-component kinetics model." *Bull. Chem. React. Eng. Catal. 18*, 85-102.

Widawati, T.F., Refki, M.F., Rochmadi, Wintoko, J., & Budiman, A., 2024. "Comprehensive study of lumped kinetic models and bio-oil characterization in microwave-assisted pyrolysis of *Sargassum* sp". *React. Chem. Eng*. *9*, 1959-1980.

Yadav A., Ansari K.B., Simha, P., Gaikar, V.G., and Pandit, A.B., 2016. "Vacuum pyrolyzed biochar for soil amendment." *Resource-Efficient Technologies 2*, S177-S185.

Yang, C., Li, R., Zhang, B., Qiu, Q., Wang, B., Yang, H., and Wang, C., 2019. "Pyrolysis of microalgae: A critical review." *Fuel Process. Technol*. *186*, 53–72.

Yao, Y., Jänis, A., and Klement, U., 2008. "Characterization and dielectric properties of β-SiC nanofibres." *J. Mater. Sci. 43*, 1094–1101.

Yusuf, J. Y., Soleimani, H., Yahya, N., Sanusi, Y. K., Kozlowski, G., Öchsner, A., Adebayo, L. L., Wahaab, F. A., Sikiru, S., and Balogun, B. B., 2022. "Electromagnetic wave absorption of coconut fiber-derived porous activated carbon." *Boletin de La Sociedad Espanola de Ceramica y Vidrio 61*, 417–427.

Zhang, Y., Chen P., Liu, S., Fan, L., Zhou, N., Min, M., Cheng, Y., Peng, P., Anderson, E., Wang, Y., Wan, Y., Liu, Y., Xi, B., and Ruan, R., 2017. Microwave-Assisted Pyrolysis of Biomass for Bio-Oil Production. Samer, M., ed., *Pyrolysis*. IntechOpen, London.

Zhang, Y., Liang, Y., Li, S., Yuan, Y., Zhang, D., Wu, Y., Xie, H., Brindhadevi, K., Pugazhendhi A., and Xia, C., 2023. "A review of biomass pyrolysis gas: Forming mechanisms, influencing parameters, and product application upgrades." *Fuel 347*, 128461.

Zhou, N., Dai, L., Lyu, Y., Li, H., Deng, W., Guo, F., Chen, P., Lei, H., and Ruan, R., 2021. "Catalytic pyrolysis of plastic wastes in a continuous microwave assisted pyrolysis system for fuel production." *Chem. Eng. J. 418*, 129412.